sciendo

POLISH MARITIME RESEARCH 2 (118) 2023 Vol. 30; pp. 61-67
10.2478/pomr-2023-0021

HIGH QUALITY MULTI-ZONE AND 3D CFD MODEL OF COMBUSTION IN MARINE DIESEL ENGINE CYLINDER

Dominika Cuper-Przybylska [1]
Van Nhanh Nguyen [2]
Cao Dao Nam [3]
Jerzy Kowalski [4*]

[1] Central Office of Measures POLAND, Poland
[2] Institute of Engineering, HUTECH University, Ho Chi Minh City, Viet Nam
[3] Institute of Mechanical Engineering, Ho Chi Minh City University of Transport, Ho Chi Minh City, Viet Nam
[4] Gdansk University of Technology, Poland

* Corresponding author: *jerzy.kowalski@pg.edu.pl (J. Kowalski)*

ABSTRACT

The paper presents a 3D model of the processes taking place in the cylinder of a large 4-stroke marine engine. The model is based on CFD calculations performed on the moving mesh. The modelling range includes the full duty cycle (720° crankshaft position) and the complete geometry of the cylinder with inlet and exhaust ducts. The input data, boundary conditions and validation data were obtained by direct measurements on the real object. Fuel injection characteristics were obtained by Mie scattering measurements in a fixed-volume chamber. The modelling results have been validated in terms of the pressure characteristics of the engine's cylinder within the entire range of its loads. The mean error did not exceed 1.42% for the maximum combustion pressure and 1.13% for the MIP (Mean Indicated Pressure). The model was also positively validated in terms of the O_2 and NO_X content of the exhaust gas. The mean error in this case was 1.2% for NO_X fractions in the exhaust gas and 0.4% for O_2 fractions. The complete model data has been made available in the research data repository on an open access basis.

Keywords: CFD combustion model, large 4-stroke engine, diesel engine, emission, NO_X concentration

INTRODUCTION

Proper evaluation of the processes taking place in the piston engine cylinder is necessary for the design of structures with high energy and environmental performance. A mathematical model, the results of which are verified by real-world measurements, is used increasingly often. This model enables modification of the engine design to improve its performance without incurring significant financial expenses for experimental research. CFD models based on FEM are a common class of models used for this purpose and the use of these types of models in design is basically a standard. It should be noted, however, that the mathematical description of the phenomena occurring in the engine combustion chamber for the modelling of the exhaust gas composition is very complex. During the operation of the diesel engine, injection, spraying and evaporation of the fuel, fuel mixing with air, self-ignition, combustion and turbulent propagation of flame occur simultaneously in the combustion chamber. In addition, the thermodynamic conditions of these phenomena are determined by the movement of the piston, the movement of the valves and the exchange of heat with the engine components. Therefore, despite significant advances in information technology, such models are a kind of compromise between the simplicity of the model and the accuracy of the modelling results.

Because the modelling of the key phenomena requires considerable computer resources, combustion process models are often greatly simplified [1]. Unfortunately, the simplifications used so far to assess the composition of exhaust gases, such as the limitation of the size of the mesh [2], 0-, 1- and 2-dimensional

models [2–4], or the simplified description of combustion phenomena [5–6], etc., result in significant discrepancies between the calculation results and the values measured.

Due to limited computer resources, most of the research available in the literature concerns the design of engine sizes that are relatively small in relation to marine engines [7]. The design of marine engines is different from the design of small engines. The most important differences are the cubic capacity of 10–30 litres per cylinder, the speed below 1,500 rpm, the extended piston stroke, the high boost pressure, the start of ignition before the upper dead point of the piston, and the operation of the engine at a constant speed or according to the propeller characteristics [8].

These differences between relatively small engines and those used in shipbuilding produce significant changes in the measured thermodynamic parameters and in the composition of the exhaust gases. Sarvi *et al.* [9] presented an extensive study in which they set out the characteristics of exhaust gas emissions from a large medium-speed compression ignition engine with a design similar to that used in shipbuilding. According to their findings, an increase in engine load when operating at a constant speed results in a reduction in NO_X emissions. This trend is the inverse of the emission characteristics presented for a relatively small engine [10]. In both cases, a reduction in the engine speed resulted in an increase in NO_X emissions [11–13]. The marine engine load parameters, similar to fixed pitch propeller conditions, cause varied changes in NO_X emissions [14].

In principle, it is possible to find only relatively few 3D CFD models of the combustion processes taking place in piston engines with dimensions and thermodynamic parameters similar to marine engines. The author of [15] used a simplified 0-dimensional heat evolution model for a large-capacity 2-stroke engine. A multi-zone combustion model for a marine engine is also presented in [16], but it is not a model that reproduces the shape of the whole 3D combustion chamber. A model of mean values for a marine engine was presented by Alegret *et al.* [17] to assess the impact of the bypass valve and the EGR system on engine operation. On the other hand, comprehensive multidimensional models are available only for relatively small designs [18–19].

For these reasons, the aim of this study was to build 3D and CFD models of the phenomena occurring in the cylinder of a marine 4-stroke diesel engine for assessment of the composition of the exhaust gases. The presented model is unique in the research literature due to its complexity and suitability for the modelling of large marine engines. This model is available for use on an open access basis in the scientific data repository of Gdansk University of Technology [20].

EXPERIMENT – INPUT DATA AND DATA FOR MODEL VERIFICATION

To achieve our goal, input data needs to be collected to identify the model and to verify the modelling results. For this purpose, laboratory tests on a direct-injection 3-cylinder turbocharged 4-stroke diesel engine were carried out. The test bench layout is shown in Fig. 1 and the basic specifications of the Sulzer 3AL25/30 engine are provided in Table 1.

Tab. 1. Specifications of the Sulzer 3AL25/30 engine

Parameter	Unit	Value
MIP max	MPa	1.15
Speed	rpm	750
Number of cylinders	–	3
Bore	mm	250
Stroke	mm	300
Cylinder capacity	dm^3	14.7
Compression ratio	–	12.7
Injector		
Number of nozzles	–	9
Nozzles diameter	mm	0.325
Open pressure	MPa	25

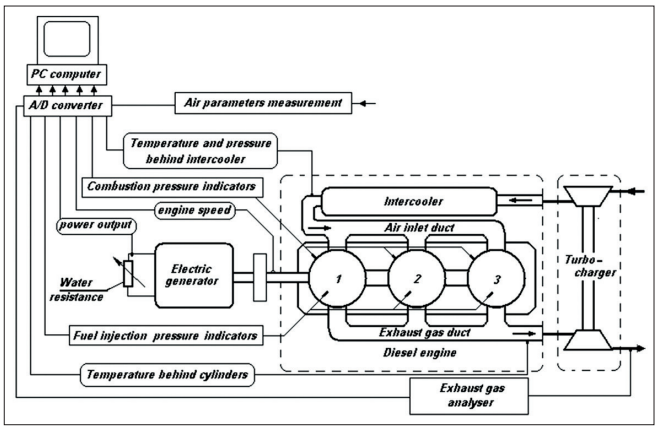

Fig. 1. Layout of the measuring station [21]

During the tests, the engine was charged using a generator electrically connected to a water resistor. A charge air cooler was also used. During the measurements the engine was powered by diesel oil of a known specification. The fuel apparatus of the engine consisted of mechanically controlled Bosch-type pumps combined with multiple-hole injectors. The engine design presented is commonly used on ships as the propulsion of generators or as the main propulsion of the ship together with the variable-pitch propeller [8]. Fifty-six laboratory station parameters were measured during the tests, including the engine speed and load, the speed of the turbocharger and the temperatures and pressures of the cooling water, lubricating oil, charge air, exhaust gas and fuel parameters. Exhaust gases were analysed using an electrochemical analyser with an infrared sensor to measure the CO_2 fractions. The air humidity, temperature, and pressure were also measured. The air flow rate was measured using a Venturi orifice to determine the emissions of exhaust gas ingredients. All these parameters were measured with a sampling time of 1 second. The engine cylinder pressure and fuel pressure in the fuel lines in front of the injectors were measured with a resolution equal to 0.5° of the rotation of the

crankshaft. Fuel consumption was measured by the volumetric method. A detailed description of the tests and their results can be found, e.g., in [21].

MODELLING

THE MOVING MESH

The building of the moving mesh of the engine cylinder requires a compromise between the accuracy of the representation of the phenomena occurring in the engine cylinder and the calculation time. Increasing the size of the finite volumes used in the mesh reduces the required processing power but also the accuracy of the modelling. This problem is particularly important in the case of modelling combustion processes in relatively large marine engines. Assuming that the mean diameter of the droplets of fuel injected into the cylinder is in the order of 10–50 μm [5] and that the cylinder diameter is 250 mm, it is necessary to create a moving mesh consisting of about 10^{15} finite volumes. This size, combined with the complexity of the phenomena occurring in the engine cylinders, would result in calculation times measured in weeks or months, however, even using the latest computation servers. Therefore, the number of finite elements was reduced to 10^6, which shortened the computation time for a single cycle of the 4-stroke engine (720° crankshaft position), using 32 CPU cores and 192 GB RAM, to about 500 hours. The mesh, presented schematically in the form of sections in Fig. 2, occupies a storage space exceeding 8 GB.

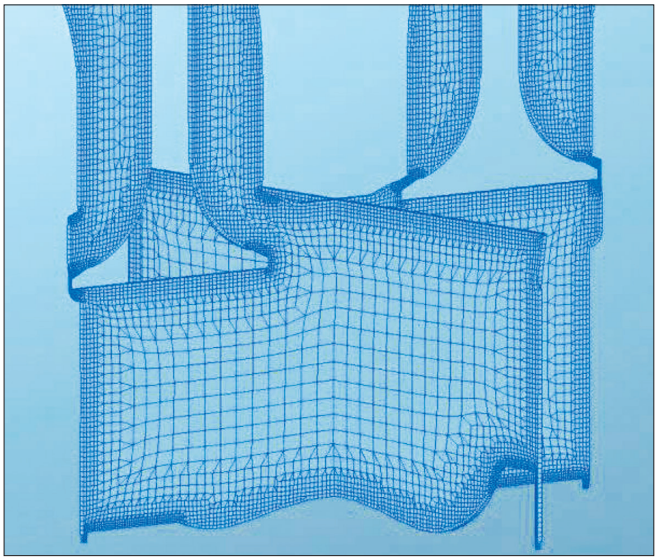

Fig. 2. Diagram of the moving mesh

To analyse the calculation time, three moving meshes were defined, from which the optimal solution was ultimately selected. The course of the mesh preparation is described in [22]. This mesh consists of 500,000 finite volumes for the combustion chamber and 1,500,000 finite volumes when the inlet and outlet ducts are opened during the modelling of the working medium replacement. The maximum finite volume size of 8 mm was used. In places where there was intensification of the modelled phenomena (fuel injection, ignition, high flow rate, turbulence, etc.), the size of the finite volumes was limited to 1–2 mm. The size of the finite volumes of the moving mesh also required a compaction to a dimension equal to 0.125 mm in the vicinity of the valve faces, at the time of opening and closing. Examples of the densities are shown in Fig. 3. This mesh allowed the full engine cycle to be calculated using 25,110 iterations. The mesh and the complete configuration files are provided in the open access data [20] and the calculation performance analysis using this grid in [22].

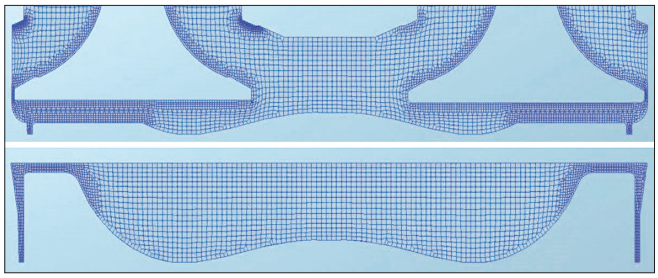

Fig. 3. Perpendicular sections in the mesh at the time of flushing

FUEL INJECTION

The building of the model of the delivery of fuel to the cylinder requires determination of the shape of the fuel jet and its quantitative characteristics.

The shape of the injected fuel jet was determined experimentally. The tests consisted in installing the injector in the fixed-volume chamber filled with nitrogen to the pressures of 3.2 and 4.3 MPa. These pressures correspond to the pressure in the engine cylinder at the start of the fuel injection for the minimum load and the maximum load, respectively. Fuel was delivered to the injector at a constant pressure of 50 MPa, with the injector opening pressure set at 25 MPa (see Table 1). The injection flow was recorded using the Mie scattering method [23–24] with a sampling rate of 40 kHz and a resolution of 512 x 256 pixels. The detailed course of the tests and the results are presented in [25].

The quantitative characteristics of the fuel injection depend on the injection start time and on its progress in time. In the classic self-ignition engine fuel apparatus design, the start of fuel injection into the cylinders is constant and depends on the angular position of the camshaft. This time was identified by determining the change in the fuel level in the transparent vertical tube mounted directly on the fuel pump during the slow rotation of the shaft. The reading was made with an accuracy of 0.5° of the crankshaft position. As a result of the observations made, the angle of the start of the fuel injection into the cylinders was set at 18° bTDC. The mass flow rate of the fuel injection into the cylinder was determined based on an analysis of the fuel pressure characteristics measured on the fuel lines before the injectors of the test facility. Assuming a constant flow rate from the nozzle, it can be assumed that the mass flow rate of the fuel is directly proportional to the pressure in the fuel line. This solution was proposed due to

the lack of technical possibilities to install an injector needle position sensor.

COMBUSTION

The fuel supplied to the engine cylinder is sprayed and evaporated. The WAVE model [26] along with the modification by Wakisaki [27] and Dukowicz's evaporation model [28] were used. The TAB [29], Chu [30] and FIPA [31] models were also taken into account but the verification of the calculation results led to their rejection.

Many models of combustion processes are described in the literature on the subject, but the most popular models in the last 15 years are based on Coherent Flame Models [32]. These models describe the combustion process on the assumption that the scale of the chemical reactions is many times smaller than the phenomena associated with the turbulent mass flow of the gas mixture in the engine cylinder. This assumption allows for a separate description of both phenomena. This approach was used by Colin and Benkenida [12]. The model modified by these authors, called the 3-Zones Extended Coherent Flame Model (ECFM-3Z or 3Z-ECFM), allows for correct combustion process modelling results for compression ignition engines. This model has been positively verified, e.g., in studies [33–38], and assumes that ignition and combustion take place in a certain volume containing a homogeneous mixture of fuel and air. The proportions of the mixture are determined based on the results of calculations using equations of the turbulent mixing of evaporated fuel with air and the resulting mixture with air and combustion products. This model also determines the delay of the self-ignition. The flame propagation in the combustion chamber is also described in the 3Z-ECFM model, with the flame areas being defined by the emission model based on fuel oxidation reactions.

Thus, in the proposed model, fuel with the accepted substitute composition of the $C_{13}H_{23}$ hydrocarbons, evaporating according to Dukowicz's model, is mixed with air in the cylinder space. The quantity and composition of the mixture in each finite volume of the moving mesh are calculated based on the averaged Navier–Stokes and flow continuity equations. The Reynolds Averaged Navier–Stokes equations (RANS) method was chosen due to its relatively short computation time. The k-zeta-f model proposed by Hanjalyc, Popovac and Hadziabdic in 2004 [39] was used to average the turbulent flow in the finite volumes. This iterative SIMPLE calculation algorithm [40] was used to correct the pressures in the finite volumes. Under-relaxation factors were selected for each of the balance equations considered and for each crankshaft position. The selection of these factors allowed for correct results in no more than 100 iterations for each equation, with an assumed calculation accuracy of 1%. Methods for solving first-order hyperbolic equations in the form of the "upwind" differential scheme [41] were used to calculate the energy balances and turbulent flows, and the central differential scheme [42] was applied to the calculation of the flow continuity equations. A variable calculation step was also defined. During the compression stroke the calculation step was equal to 1° of the crankshaft position. This step was reduced to 0.02° when the fuel was sprayed, ignited and when the outlet valve was opened.

This study used the combination of two NO_X formation mechanisms: Zeldowicz's thermal mechanism and Fenimore's mechanism of quick nitrogen oxides. Other NO_X formation mechanisms, including the mechanism of formation from the nitrogen contained in the fuel, were omitted due to the negligible nitrogen content in the fuel used.

HEAT EXCHANGE MODEL

The course of the phenomena occurring in the engine cylinders during the combustion process depends on the prevailing thermodynamic conditions. These, in turn, result from the combustion process itself and from the exchange of heat with the structural elements of the cylinders [43].

In the presented combustion process model, the heat transfer model is implemented into each finite volume located on the outer surfaces of the mobile mesh. Boundary conditions of the third type [44] were applied in the form of the determination of the heat flow rate through the structural components of the engine cylinder to the cooling system due to radiation and heat conduction. Fixed values for the heat take-over factor, $\alpha=3.5\bullet10^4$ W/(m²•K), thermal resistance, R=37 (m²•K)/W, and emissivity, $\varepsilon=0.79$, were adopted. It should be borne in mind that the values of these coefficients depend, inter alia, on the temperature of the combustion process, the specific heat and viscosity of the mixture in the cylinder, as well as the speed of flows. However, the introduction of these dependencies would require an additional iterative loop to be introduced into the calculation algorithm to determine the temperature of the cylinder walls. The result would be a significant increase in the computation time. The calculations described were done with the AVL Fire package.

The complete model data has been made available in the research data repository on an open access basis, as a tool to be used in research by a wide range of scientists [20].

MODELLING RESULTS AND VALIDATION

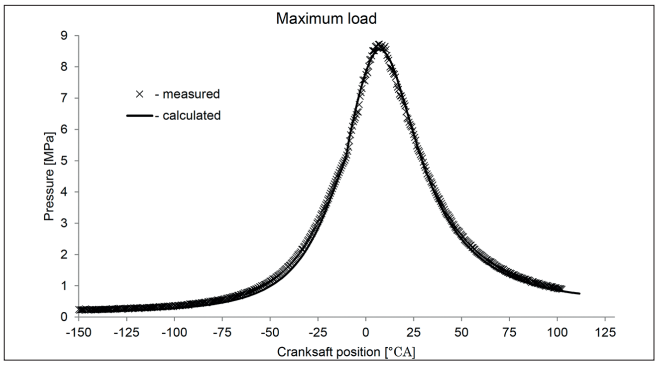

Fig. 4. Calculated combustion pressure and measured engine cylinder pressure for the maximum load

Fig. 4 illustrates an example of the combustion pressure characteristics in a cylinder, obtained by modelling and by direct measurements. The continuous line shows the results obtained by calculation. An example visualisation of the

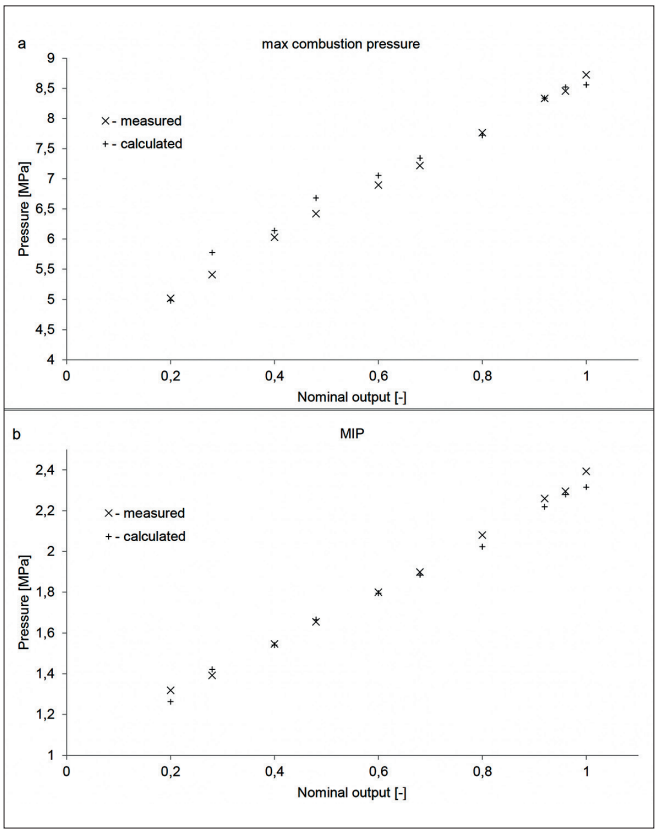

Fig. 5. Calculated and measured (a) max. pressure and (b) MIP in engine cylinders

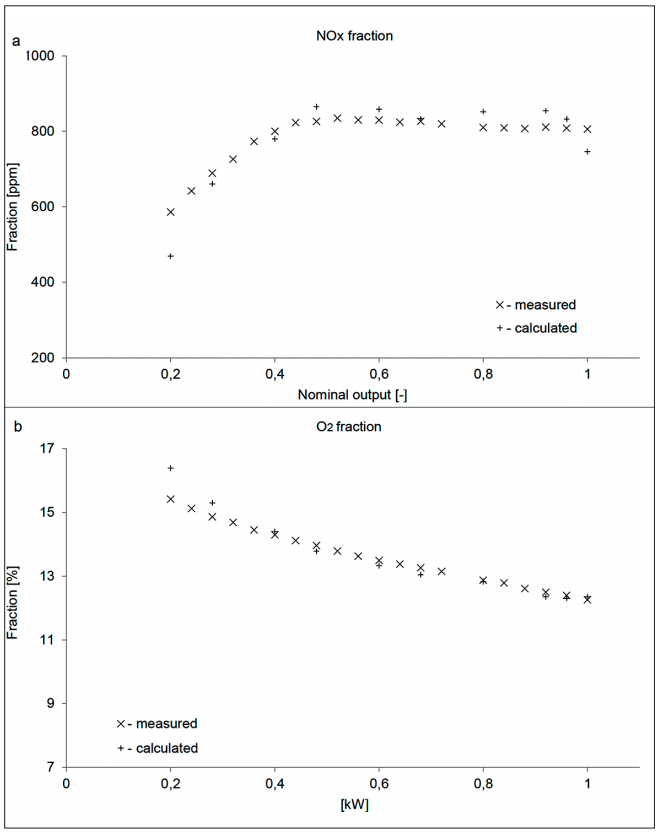

Fig. 6. Calculated and measured fractions of (a) NO_X and (b) O_2 in combustion gases

temperature distribution in the engine cylinder during fuel injection with a self-ignition focus is also shown. Fig. 5 presents the aggregate results of the calculations and measurements of the combustion pressure in the engine cylinders. A comparison was made between the calculated and measured MIP values and the maximum combustion pressure. According to the above results, the largest relative error for MIP, 4.3%, was achieved for a test facility load of 50 kW. The mean error in the values calculated in relation to the values measured for the entire load range considered for the test facility was 1.42% for the maximum pressure and 1.13 % for the MIP, respectively.

The results of the calculations obtained were also validated based on the composition of the exhaust gases emitted. Fig. 6 shows the results of the calculations and measurements of the NO_X and O_2 fractions in the exhaust gases of the test facility, being recognised as efficient. According to the results presented, the mean error in the values calculated in relation to the values measured for the whole engine load range equals 1.2% for the NO_X fractions in the exhaust gases and 0.4% for the O_2 fractions. It should be noted that, in this case too, the largest calculation errors were obtained for the minimum engine load considered.

The accuracy of the exhaust gas analyser measuring lines used in the experimental tests was used as a criterion for accepting the validation of the results for the NO_X and O_2 fractions. This accuracy is 5% of the indication for the NO_X probe and 0.2% of the absolute O_2 fractions in the exhaust gas. According to the considerations presented, the modelling results in Fig. 6 fall within the established validation criterion.

CONCLUSIONS

The aim of the study was to build a model of the combustion process of a 4-stroke marine engine. For this purpose, a moving mesh was built covering the cylinder space and the inlet and outlet ducts. The model is based on partial models including the WAVE fuel spraying model, Dukowicz's fuel evaporation model and the 3Z-ECFM combustion model. The initial and boundary conditions and data necessary for the validation of the calculation results were obtained by direct experimental measurements. As a result of the work carried out, it was possible to create a model mapping the fractions of NO_X and O_2 in exhaust gases.

The validation results presented allow the use of the resulting model to look for relations between the parameters of the combustion process in a 4-stroke marine engine and the composition of the exhaust gases. This model calculates the NO_X and O_2 fractions with an accurate quantitative analysis. According to the results presented, the mean error in the values calculated in relation to the values measured for the entire engine load range considered was 1.2% for the NO_X fractions in the exhaust gases and 0.4% for the O_2 fractions. The model has also been successfully validated in terms of the pressure characteristics of the engine cylinder during the combustion process. The complete model data has been made available in the research data repository on an open access basis, as a tool to be used in research by a wide range of scientists.

CREDITS

The work was supported by AVL, the FIRE software developer, under the "University Partnership" affiliate program.

REFERENCES

1. M. H. Ghaemi, "Performance and emission modelling and simulation of marine diesel engines using publicly available engine data," *Polish Maritime Research*, vol. 28(4), pp. 63–87, 2021. https://doi.org/10.2478/pomr-2021-0050

2. J. Shu, J. Fu, J. Liu, Y. Ma, S. Wang, B. Deng, and D. Zeng, "Effects of injector spray angle on combustion and emissions characteristics of a natural gas (NG)-diesel dual fuel engine based on CFD coupled with reduced chemical kinetic model," *Applied Energy*, vol. 233–234, pp. 182–195, 2019. https://doi.org/10.1016/j.apenergy.2018.10.040

3. T. Poinsot and D. Veynante, *Theoretical and numerical combustion*. Edwards, 2005.

4. F. Payri, P. Olmeda, J. Martín, and A. García, "A complete 0D thermodynamic predictive model for direct injection diesel engines," *Applied Energy*, vol. 88, pp. 4632–4641, 2011. https://doi.10.1016/j.apenergy.2011.06.005

5. K. K. Kuo, *Principles of combustion*. New Jersey, Wiley, 2005.

6. S. Wang and L. Yao, "Effect of engine speeds and dimethyl ether on methyl decanoate HCCI combustion and emission characteristics based on low-speed two-stroke diesel engine," *Polish Maritime Research*, vol. 27(2), pp. 85–95, 2020. https://doi.org/10.2478/pomr-2020-0030

7. H. Eichlseder and A. Wimmer, "Potential of IC-engines as minimum emission propulsion system," *Atmos. Environ.*, vol. 37(37), pp. 5227–5236, 2003. https://doi.org/10.1016/j.atmosenv.2003.05.001

8. J. Carlton, *Marine Propellers and Propulsion*, 3rd ed. Elsevier Ltd., 2012.

9. A. Sarvi, C. J. Fogelholm, and R. Zevenhoven, "Emissions from large-scale medium-speed diesel engines: 1. Influence of engine operation mode and turbocharger," *Fuel Processing Technology*, vol. 89, pp. 510–519, 2008. https://doi.org/10.1016/j.fuproc.2007.10.006

10. D. Agarwal, S. K. Singh, and A. K. Agarwal, "Effect of exhaust gas recirculation (EGR) on performance, emissions, deposits and durability of a constant speed compression ignition engine," *Applied Energy*, vol. 88, pp. 2900–2907, 2011. https://doi.org/10.1016/j.apenergy.2011.01.066

11. A. Sarvi, C. J. Fogelholm, and R. Zevenhoven, "Emissions from large-scale medium-speed diesel engines: 2. Influence of fuel type and operating mode," *Fuel Processing Technology*, vol. 89, pp. 520–527, 2008. https://doi.org/10.1016/j.fuproc.2007.10.005

12. O. Colin and A. Benkenida, "The 3-zones extended coherent flame model (ECFM3Z) for computing premixed/diffusion combustion," *Oil & Gas Science and Technology*, vol. 59(6), pp. 593–609, 2004. https://doi.org/10.2516/ogst:2004043

13. C. Rodriguez, M. Lamas, J. Rodriguez, and A. Abbas, "Analysis of the pre-injection system of a marine diesel engine through multiple-criteria decision-making and artificial neural networks," *Polish Maritime Research*, vol. 28(4), pp. 88–96, 2021. https://doi.org/10.2478/pomr-2021-0051

14. Z. Korczewski, "Test method for determining the chemical emissions of a marine diesel engine exhaust in operation," *Polish Maritime Research*, vol. 28(3), pp. 76–87, 2020. https://doi.org/10.2478/pomr-2021-0035

15. Z. Yang, Q. Tan, and P. Geng, "Combustion and emissions investigation on low-speed two-stroke marine diesel engine with low sulfur diesel fuel," *Polish Maritime Research*, vol. 26(1), pp. 153–161, 2011. https://doi.org/10.2478/pomr-2019-0017

16. R. Zhao, L. Xu, X. Su, S. Feng, C. Li, Q. Tan, and Z. Wang, "A numerical and experimental study of marine hydrogen–natural gas–diesel tri-fuel engines," *Polish Maritime Research*, vol. 27(4), pp. 80–90, 2020. https://doi.org/10.2478/pomr-2020-0068

17. G. Alegret, X. Llamas, M. Vejlgaard-Laursen, and L. Eriksson, "Modeling of a large marine two-stroke diesel engine with cylinder bypass valve and EGR system," *IFAC-PapersOnLine*, vol. 48(16), pp. 273–278, 2015. https://doi.org/10.1016/j.ifacol.2015.10.292

18. F. Payri, J. Benajes, X. Margot, and A. Gil, "CFD modeling of the in-cylinder flow in direct-injection diesel engines," *Computers & Fluids*, vol. 33, pp. 995–1021, 2004. https://doi.org/10.1016/j.compfluid.2003.09.003

19. Z. Sahin and O. Durgun, "Multi-zone combustion modeling for the prediction of diesel engine cycles and engine performance parameters," *Applied Thermal Engineering*, vol. 28, pp. 2245–2256, 2008. https://doi.org/10.1016/j.applthermaleng.2008.01.002

20. J. Kowalski, *Complete input data to CFD 3D model of combustion in the large marine 4-stroke engine*, 2018. [Dataset]. https://doi.org/10.34808/0kbc-ny83.

21. J. Kowalski, "An experimental study of emission and combustion characteristics of marine diesel engine with fuel pump malfunctions," *Appl. Therm. Eng.*, vol. 65(1–2), pp. 469–79, 2014. https://doi.org/10.1016/j.applthermaleng.2014.01.028

22. J. Kowalski and P. Jaworski, "3D mesh model for RANS numerical research on marine 4-stroke engine," *Journal of Polish CIMAC*, vol. 9(1), pp. 87–94, 2014.

23. S. N. Soid and Z. A. Zainal, "Spray and combustion characterization for internal combustion engines using optical measuring techniques – A review," Energy, vol. 36(2), pp. 724–741, 2011. https://doi.org/10.1016/j.energy.2010.11.022

24. E. Delacourt, B. Desmet, and B. Besson, "Characterisation of very high pressure diesel sprays using digital imaging techniques," *Fuel*, vol. 84(7–8), pp. 859–867, 2005. https://doi.org/10.1016/j.fuel.2004.12.003

25. J. Grochowalska, J. Kowalski, Ł. J. Kapusta, and P. Jaworski, *The experimental results of diesel fuel spray with marine engine injector*, 2021. [Dataset]. https://doi.org/10.34808/c3aw-dq41.

26. A. B. Liu and R. D. Reitz, *Modeling the Effects of Drop Drag and Break-up on Fuel Sprays*. SAE Technical Paper. 1993; 930072.

27. T. Wakisaka et al., *Numerical Prediction of Mixture Formation and Combustion Processes in Premixed Compression Ignition Engines*. COMODIA, 2001.

28. J. K. Dukowicz, *Quasi-steady droplet change in the presence of convection*. Informal Report, Los Alamos Scientific Laboratory, LA7997-MS.

29. P. O'Rourke and A. Amsden, *The TAB Method for Numerical Calculation of Spray Droplet Breakup*. SAE Technical Paper, 1987, 872089.

30. C. C. Chu and M. L. Corradini, "One-dimensional transient fluid model for fuel/coolant interaction analysis," *Nuclear Science and Engineering*, vol. 101, pp. 48–71, 1989.

31. C. Habchi and D. Verhoeven, *Modeling Atomization and Break Up in High-Pressure Diesel Sprays*. SAE Technical Paper, 1997, 970881.

32. F. E. Marble and J. E. Broadwell, *The Coherent Flame Model for Turbulent Chemical Reactions*. Technical Report TRW-29314-6001-RU-00, USA, 1977.

33. R. Mobasheri, Z. Peng, and S. M. Mirsalim, "Analysis the effect of advanced injection strategies on engine performance and pollutant emissions in a heavy duty DI-diesel engine by CFD modeling," *International Journal of Heat and Fluid Flow*, vol. 33, pp. 59–69, 2012. https://doi.org/10.1016/j.ijheatfluidflow.2011.10.004

34. R. Mobasheri and Z. Peng, "CFD investigation into diesel fuel injection schemes with aid of homogeneity factor," *Computers & Fluids*, vol. 77, pp. 12–23, 2013. https://doi.org/10.1016/j.compfluid.2013.02.013

35. H. Taghavifar, S. Khalilarya, and S. Jafarmadar, "Engine structure modifications effect on the flow behavior, combustion, and performance characteristics of DI diesel engine," *Energy Conversion and Management*, vol. 85, pp. 20–32, 2014. https://doi.org/10.1016/j.enconman.2014.05.076

36. S. Jafarmadar, "Exergy analysis of hydrogen/diesel combustion in a dual fuel engine using three-dimensional model," *International Journal of Hydrogen Energy*, vol. 39, pp. 9505–9514, 2014. https://doi.org/10.1016/j.ijhydene.2014.03.152

37. W. Park, J. Lee, K. Min, J. Yu, S. Park, and S. Cho, "Prediction of real-time NO based on the in-cylinder pressure in diesel engines," in *Proc. of the Combustion Institute*, vol. 34, pp. 3075–3082, 2013. https://doi.org/10.1016/j.proci.2012.06.170

38. R. Lebas, T. Menard, P. A. Beau, A. Berlemont, and F. X. Demoulin, "Numerical simulation of primary break-up and atomization: DNS and modelling study," *International Journal of Multiphase Flow*, vol. 35, pp. 247–260, 2009. https://doi.org/10.1016/j.ijmultiphaseflow.2008.11.005

39. K. Hanjalić, M. Popovac, and M. Hadžiabdić, "A robust near-wall elliptic relaxation eddy-viscosity turbulence model for CFD," *International Journal of Heat and Fluid Flow*, vol. 25(6), pp. 1047–1051, 2004. https://doi.org/10.1016/j.ijheatfluidflow.2004.07.005

40. B. Kaludercic, "Parallelisation of the Lagrangian model in a mixed Eulerian–Lagrangian CFD algorithm," *J. Parallel Distrib. Comput.*, vol. 64(2), pp. 277–284, 2004. https://doi.org/10.1016/j.jpdc.2003.11.010

41. J. Donea and A. Huerta, *Finite Element Methods for Flow Problems*. Wiley, 2003.

42. R. W. Lewis, P. Nithiarasu, and K. N. Seetharamu, *Fundamentals of the Finite Element Method for Heat and Fluid Flow*. Wiley, 2004.

43. R. J. Goldstein, W. E. Ibele, and S. V. Patankar, "Heat transfer – A review of 2003 literature," *Int. J. Heat Mass Transf.*, vol. 49(3–4), pp. 451–534, 2006. https://doi.org/10.1016/j.ijheatmasstransfer.2005.11.001

44. F. P. Incropera and D. P. DeWitt, *Fundamentals of Heat and Mass Transfer*. Wiley, 2001.